injuries to the anterior root have been demonstrated to produce mislocalisation of TDP-43 in spinal motoneurons.[41] These considerations suggest an L5 segmental vulnerability to ALS lesions, but among cervical segments, the segment C8 innervating FDI which is the most vulnerable in ALS,[7 9 10 34] is different from the segment that is commonly affected in cervical spondylosis.[42]

Kiernan and his colleagues have reported that cortical hyperexcitability is an early feature in ALS, and UMN and LMN dysfunction coexists.[43] We cannot take account of the influence of UMN impairments by spontaneous EMG activities we have investigated, hence we reviewed the clinical UMN features of the 14 patients who showed 'non-contiguous pattern' at nEMG examination (see online supplementary table S1). We can assume that they should show UMN features in both onset and lumbosacral regions if the non-contiguous pattern of nEMG is driven by the preceding UMN involvements. However, our results showed no UMN features were revealed in cervical regions in five patients (patients 23, 24, 30, 32, 35) and in lumbosacral regions in three patients (patients 24, 30, 33), neither. This result indicates the existence of some skipping mechanisms of LMN involvements regardless of UMN in propagation of ALS. On the other hand, UMN features were widespread in the rest of the patients of non-contiguous pattern. Especially, hyperreflexia was simultaneously shown in both patella tendon (quadriceps femoris; L3/4) and Achilles tendon (GC and soleus; S1) to almost the same degree even in the patients with L3/4 skipping pattern. From these findings, we could not indicate that cortical hyperexcitability is driving the non-contiguous spread of LMN involvement in ALS. However, it is well documented that cortical hyperexcitability evaluated by short intracortical inhibition with threshold tracking transcranial magnetic stimulation techniques precedes clinical UMN features,[43] which is supported by the neuropathological examination that 50% of progressive muscular atrophy patients had pyramidal tract degeneration.[44] Therefore, more detailed electrophysiological analysis is needed for elucidating the role of upper motor neuron dysfunction on this non-contiguous spread, because it is a potential target of therapeutic intervention, especially riluzole.[45 46]

FPs are considered to appear in the muscles which are in the earlier stage of involvement and are involved more slightly, especially the muscles which is located away from onset region, while Fib/PSWs tend to appear later than FPs and tend to appear in the onset muscle.[32 33 47] The fact that only L5 innervating muscles in the lumbosacral regions show Fib/PSWs less rarely than FPs suggests that L5 segment is involved at first in the lumbosacral regions and then neighbouring segments are subsequently involved.

We also analysed the anatomical distribution of the involved motoneuron pools of the lumbosacral segments in the eight patients with non-contiguously affected lumbosacral lesions. The involved motoneuron pools were located in close proximity to one another horizontally or radially, appearing to form a cluster in four patients. Local propagation of pathology between motor columns can exist after the second hit in the lumbosacral cord following the first hit at the rostral onset site (see online supplementary figure S3B). If it is true, for explanation for horizontal spread between distinct motor columns, we have to assume a different mechanism from neuron-to-neuron protein transfer; for example, diffusion of a secreted toxic soluble factor or glia-to-neuron interaction which is known in the mutant SOD1 transgenic mouse[48] may play a role in a transmission between motor columns.

In conclusion, the results of our prospective study and detailed nEMG results in 36 ALS patients showed that LMN involvement in many early stage ALS patients was distributed non-contiguously in the rostrocaudal direction of the spinal segments, indicating that the onset site is not single even with consideration of difference in motoneuronal vulnerability. On the other hand, local involvements of the anterior horn lesions tended to be formed as some clusters, and therefore, we here propose 'multifocal hits and local propagation' as a new hypothesis for one of the mechanisms of ALS progression.

Author affiliations
[1]Department of Neurology and Neurological Science, Graduate School, Tokyo Medical and Dental University, Tokyo, Japan
[2]Clinical Laboratory, Tokyo Medical and Dental University Hospital of Medicine, Tokyo, Japan
[3]Department of Neurology, Graduate School of Medicine, Chiba University, Chiba, Japan
[4]Department of Neurology, Graduate School of Medical Science, Kyoto Prefectural University of Medicine, Kyoto, Japan
[5]Department of Neurology, Musashino Red Cross Hospital, Tokyo, Japan
[6]Department of Neurology, Kanto Central Hospital, Tokyo, Japan
[7]Department of Neurology, Nakano General Hospital, Tokyo, Japan

Acknowledgements We sincerely thank Dr Nobuo Sanjo, Hiroyuki Tomimitsu, Takuya Ohkubo, Taro Ishiguro, Akira Machida, Makoto Takahashi, Yuji Hashimoto and Masahiko Ichijo (Department of Neurology and Neurological Science, Graduate School, Tokyo Medical and Dental University); Dr Shuta Toru (Department of Neurology, Nakano General Hospital); Dr Hiroaki Yokote (Department of Neurology, Musashino Red Cross Hospital); Dr Zen Kobayashi and Yoshiyuki Numasawa (Department of Neurology, JA Toride Medical Center); Dr Masato Obayashi (Department of Neurology, National Disaster Medical Center); Dr Minoru Kotera and Yoko Ito (Department of Neurology, Tsuchiura Kyodo Hospital); Dr Kotaro Yoshioka (Department of Neurology, Yokohama City Minato Red Cross Hospital); Dr Mutsufusa Watanabe and Dr Hiroya Kuwahara (Department of Neurology, Tokyo Metropolitan Bokutoh Hospital); Dr Osamu Tao (Department of Neurology, Ome Municipal General Hospital); and Dr Kazuaki Kanai (Department of Neurology, Graduate School of Medicine, Chiba University) for their excellent technical assistance and referral of patients.

Contributors TS, TK, KS, SM, SK and TY designed the study. TS, TK, KS, Y-iN, YY, AI and KA conducted the examinations. TS and TK performed statistical analysis. TS, TK and TY drafted the manuscript. SO, TK, TK, MN, HM and TY supervised the study. The version to be published was approved by all of the authors. TS accepts full responsibility for the data as the guarantor.

Funding This research was supported by a Grant-in-Aid for Scientific Research (A) to Yokota (#22240039); a Grant-in-Aid for Exploratory Research to Kanouchi. (#24659425); and Research on Neurodegenerative Diseases/ALS from the Ministry of Health, Labour, Welfare, Japan to Mizusawa; and Strategic Research Program for Brain Science, Field E from Ministry of Education, Culture, Sports and Technology, Japan to Mizusawa.

Competing interests None.

Patient consent Obtained.

Ethics approval The local ethics committees of Tokyo Medical and Dental University School of Medicine (No. 1091), Chiba University Graduate School of Medicine (No. 769), Kyoto Prefectural University of Medicine (No. E-367), Musashino Red Cross Hospital (No. 26), Kanto Central Hospital (No. 1 of Jan 12, 2012) and Nakano General Hospital (No. 23-005) approved this study.

Provenance and peer review Not commissioned; externally peer reviewed.

Data sharing statement The principal investigator: Teruhiko Sekiguchi has full access to all of the patients' clinical data including EMG results and takes full responsibility for the data, the accuracies of analyses and interpretation, and the conduct of the research.

REFERENCES

1 Goedert M, Clavaguera F, Tolnay M. The propagation of prion-like protein inclusions in neurodegenerative diseases. *Trends Neurosci* 2010;33:317–25.
2 Polymenidou M, Cleveland DW. The seeds of neurodegeneration: prion-like spreading in ALS. *Cell* 2011;147:498–508.
3 Grad LI, Guest WC, Yanai A, *et al*. Intermolecular transmission of superoxide dismutase 1 misfolding in living cells. *Proc Natl Acad Sci USA* 2011;108:16398–403.
4 Furukawa Y, Kaneko K, Watanabe S, *et al*. A seeding reaction recapitulates intracellular formation of Sarkosyl-insoluble transactivation response element (TAR) DNA-binding protein-43 inclusions. *J Biol Chem* 2011;286:18664–72.

5 DeJesus-Hernandez M, Mackenzie IR, Boeve BF, *et al*. Expanded GGGGCC hexanucleotide repeat in noncoding region of C9ORF72 causes chromosome 9p-linked FTD and ALS. *Neuron* 2012;72:245–56.
6 Munch C, O'Brien J, Bertolotti A. Prion-like propagation of mutant superoxide dismutase-1 misfolding in neuronal cells. *Proc Natl Acad Sci USA* 2011;108:3548–53.
7 Swash M. Vulnerability of lower brachial myotomes in motor neurone disease: a clinical and single fibre EMG study. *J Neurol Sci* 1980;47:59–68.
8 Swash M, Leader M, Brown A, *et al*. Focal loss of anterior horn cells in the cervical cord in motor neuron disease. *Brain* 1986;109:939–52.
9 Tsukagoshi H, Yanagisawa N, Oguchi K, *et al*. Morphometric quantification of the cervical limb motor cells in controls and in amyotrophic lateral sclerosis. *J Neurol Sci* 1979;41:287–97.
10 Kanouchi T, Ohkubo T, Yokota T. Can regional spreading of ALS motor symptoms be explained by prion-like propagation? *J Neurol Neurosurg Psychiatry* 2012;83:739–45.
11 Ravits J, Paul P, Jorg C. Focality of upper and lower motor neuron degeneration at the clinical onset of ALS. *Neurology* 2007;68:1571–5.
12 Ravits J, La Spada AR. ALS motor phenotype heterogeneity, focality, and spread: deconstructing motor neuron degeneration. *Neurology* 2009;73:805–11.
13 Körner S, Kollewe K, Fahlbusch M, *et al*. Onset and spreading patterns of upper and lower motor neuron symptoms in amyotrophic lateral sclerosis. *Muscle Nerve* 2011;43:636–42.
14 Fujimura-Kiyono C, Kimura F, Ishida S, *et al*. Onset and spreading patterns of lower motor neuron involvements predict survival in sporadic amyotrophic lateral sclerosis. *J Neurol Neurosurg Psychiatry* 2011;82:1244–9.
15 Rabin SJ, Kim JM, Baughn M, *et al*. Sporadic ALS has compartment-specific aberrant exon splicing and altered cell-matrix adhesion biology. *Hum Mol Genet* 2010;19:313–28.
16 Gargiulo-Monachelli GM, Janota F, Bettini M, *et al*. Regional spread pattern predicts survival in patients with sporadic amyotrophic lateral sclerosis. *Eur J Neurol* 2012;19:834–41.
17 Wohlfart G. Collateral regeneration in partially denervated muscles. *Neurology* 1958;8:175–80.
18 Brooks BR, Miller RG, Swash M, *et al*. El Escorial revisited: revised criteria for the diagnosis of amyotrophic lateral sclerosis. *Amyotroph Lateral Scler Other Motor Neuron Disord* 2000;1:293–9.
19 Haverkamp LJ, Appel V, Appel SH. Natural history of amyotrophic lateral sclerosis in a database population. Validation of a scoring system and a model for survival prediction. Brain 1995;118:707–19.
20 Cappellari A, Brioschi A, Barbieri S, *et al*. A tentative interpretation of electromyographic regional differences in bulbar- and limb-onset ALS. *Neurol* 1999;52:644–6.
21 Pun S, Santos AF, Saxena S, *et al*. Selective vulnerability and pruning of phasic motoneuron axons in motoneuron disease alleviated by CNTF. *Nat Neurosci* 2006;9:408–19.
22 Mannion AF, Weber BR, Dvorak J, *et al*. Fibre type characteristics of the lumbar paraspinal muscles in normal healthy subjects and in patients with low back pain. *J Orthop Res* 1997;15:881–7.
23 Liguori R, Krarup C, Trojaborg W. Determination of the segmental sensory and motor innervation of the lumbosacral spinal nerves: an electrophysiological study. *Brain* 1992;115:915–34.
24 Perotto AO. *Anatomical guide for the electromyographer: the limbs and trunk*, 5th edn. Springfield, IL: Charles C Thomas, 2011:21–250.
25 Wilbourn AJ, Aminoff MJ. AAEE minimonograph #32: the electrophysiologic examination in patients with radiculopathies. *Muscle Nerve* 1998;11:1099–114.
26 Tsao BE, Levin KH, Bodner RA. Comparison of surgical and electrodiagnostic findings in single root lumbosacral radiculopathies. *Muscle Nerve* 2003;27:60–4.
27 Johnson MA, Polgar J, Weightman D, *et al*. Data on the distribution of fibre types in thirty-six human muscles. An autopsy study. *J Neurol Sci* 1973;18:111–29.
28 Haig AJ, Moffroid M, Henry S, *et al*. A technique for needle localization in paraspinal muscles with cadaveric confirmation. *Muscle Nerve* 1991;14:521–6.
29 Mills KR. Detecting fasciculations in amyotrophic lateral sclerosis: duration of observation required. *J Neurol Neurosurg Psychiatry* 2011;82:549–51.
30 Routal RV, Pal GP. A study of motoneuron groups and motor columns of the human spinal cord. *J Anat* 1999;195:211–24.
31 Carpenter MB. *Human neuroanatomy*, 8th edn. Baltimore: Williams & Wilkins, 1983:252–4.
32 Krarup C. Lower motor neuron involvement examined by quantitative electromyography in amyotrophic lateral sclerosis. *Clin Neurophysiol* 2011;122:414–22.
33 de Carvalho M, Swash M. Fasciculation potentials and earliest changes in motor unit physiology in ALS. *J Neurol Neurosurg Psychiatry* 2013;84:963–8.
34 Kuncl RW, Cornblath DR, Griffin JW. Assessment of thoracic paraspinal muscles in the diagnosis of ALS. *Muscle Nerve* 1988;11:484–92.
35 Noto Y, Misawa S, Kanai K, *et al*. Awaji ALS criteria increase the diagnostic sensitivity in patients with bulbar onset. *Clin Neurophysiol* 2012;123:382–5.
36 Date ES, Mar EY, Bugola MR, *et al*. The prevalence of lumbar paraspinal spontaneous activity in asymptomatic subjects. *Muscle Nerve* 1996;19:350–4.
37 Haig AJ, Tong HC, Yamakawa KS, *et al*. The sensitivity and specificity of electrodiagnostic testing for the clinical syndrome of lumbar spinal stenosis. *Spine* 2005;30:2667–76.
38 de Carvalho MA, Pinto S, Swash M. Paraspinal and limb motor neuron involvement within homologous spinal segments in ALS. *Clin Neurophysiol* 2008;119:1607–13.
39 Yamada M, Furukawa Y, Hirohata M. Amyotrophic lateral sclerosis: frequent complications by cervical spondylosis. *J Orthop Sci* 2003;8:878–81.
40 Sakai T, Sairyo K, Takao S, *et al*. Incidence of lumbar spondylolysis in the general population in Japan based on multidetector computed tomography scans from two thousand subjects. *Spine* 2009;34:2346–50.
41 Moisse K, Volkening K, Leystra-Lantz C, *et al*. Divergent patterns of cytosolic TDP-43 and neuronal progranulin expression following axotomy: implications for TDP-43 in the physiological response to neuronal injury. *Brain Res* 2009;1249:202–11.
42 Yoss RE, Corbin KB, Maccarty CS, *et al*. Significance of symptoms and signs in localization of involved root in cervical disk protrusion. *Neurology* 1957; 7:673–83.
43 Vucic S, Kiernan MC. Novel threshold tracking techniques suggest that cortical hyperexcitability is an early feature of motor neuron disease. *Brain* 2006;129:2436–46.
44 Kim WK, Liu X, Sandner J, *et al*. Study of 962 patients indicates progressive muscular atrophy is a form of ALS. *Neurology* 2009;73:1686–92.
45 Vucic S, Lin CS, Cheah BC, *et al*. Riluzole exerts central and peripheral modulating effects in amyotrophic lateral sclerosis. *Brain* 2013;136:1361–70.
46 Stefan K, Kunesch E, Benecke R, *et al*. Effects of riluzole on cortical excitability in patients with amyotrophic lateral sclerosis. *Ann Neurol* 2001;49:536–9.
47 Okita T, Nodera H, Shibuta Y, *et al*. Can Awaji ALS criteria provide earlier diagnosis than the revised El Escorial criteria? *J Neurol Sci* 2011;302:29–32.
48 Boillée S, Yamanaka K, Lobsiger CS, *et al*. Onset and progression in inherited ALS determined by motor neurons and microglia. *Science* 2006;312:1389–92.

Human Molecular Genetics, 2013, Vol. 22, No. 20 **4136–4147**
doi:10.1093/hmg/ddt262
Advance Access published on June 4, 2013

Decreased number of Gemini of coiled bodies and U12 snRNA level in amyotrophic lateral sclerosis

Tomohiko Ishihara[1,†], Yuko Ariizumi[1,†], Atsushi Shiga[2,†], Taisuke Kato[1], Chun-Feng Tan[2], Tatsuya Sato[1], Yukari Miki[2], Mariko Yokoo[1], Takeshi Fujino[1], Akihide Koyama[3], Akio Yokoseki[1], Masatoyo Nishizawa[1,3], Akiyoshi Kakita[3,4], Hitoshi Takahashi[2,3] and Osamu Onodera[3,5,*]

[1]Department of Neurology, [2]Department of Pathology, Clinical Neuroscience Branch, [3]Center for Transdisciplinary Research, [4]Department of Pathological Neuroscience, [5]Department of Molecular Neuroscience, Resource Branch for Brain Disease Research, Center for Bioresource-based Research, Brain Research Institute, Niigata University, 1-757 Asahimachi-dori, Chuo-ku, Niigata-City, Niigata 951-8585, Japan

Received May 13, 2013; Revised May 13, 2013; Accepted May 30, 2013

Disappearance of TAR-DNA-binding protein 43 kDa (TDP-43) from the nucleus contributes to the pathogenesis of amyotrophic lateral sclerosis (ALS), but the nuclear function of TDP-43 is not yet fully understood. TDP-43 associates with nuclear bodies including Gemini of coiled bodies (GEMs). GEMs contribute to the biogenesis of uridine-rich small nuclear RNA (U snRNA), a component of splicing machinery. The number of GEMs and a subset of U snRNAs decrease in spinal muscular atrophy, a lower motor neuron disease, suggesting that alteration of U snRNAs may also underlie the molecular pathogenesis of ALS. Here, we investigated the number of GEMs and U11/12-type small nuclear ribonucleoproteins (snRNP) by immunohistochemistry and the level of U snRNAs using real-time quantitative RT-PCR in ALS tissues. GEMs decreased in both TDP-43-depleted HeLa cells and spinal motor neurons in ALS patients. Levels of several U snRNAs decreased in TDP-43-depleted SH-SY5Y and U87-MG cells. The level of U12 snRNA was decreased in tissues affected by ALS (spinal cord, motor cortex and thalamus) but not in tissues unaffected by ALS (cerebellum, kidney and muscle). Immunohistochemical analysis revealed the decrease in U11/12-type snRNP in spinal motor neurons of ALS patients. These findings suggest that loss of TDP-43 function decreases the number of GEMs, which is followed by a disturbance of pre-mRNA splicing by the U11/U12 spliceosome in tissues affected by ALS.

INTRODUCTION

TAR-DNA-binding protein 43 kDa (TDP-43)-immunopositive inclusions in neurons and glial cells are a pathological hallmark of sporadic amyotrophic lateral sclerosis (ALS) and familial ALS with *TARDBP* mutation (1–3). In normal cells, TDP-43 is ubiquitously expressed and diffusely distributed in the nucleoplasm with punctate foci (4). In contrast, in neurons and glial cells of tissues affected by ALS, TDP-43 forms cytoplasmic inclusions and disappears from the nucleus (1,2,5). TDP-43 functions in the nucleus and is essential for embryogenesis and postnatal cell survival (6–9), suggesting that a loss of TDP-43 from the nucleus underlies the pathogenesis of ALS (10). However, the nuclear function of TDP-43 has not been fully elucidated.

TDP-43 is a heterogeneous nuclear ribonucleoprotein and functions in RNA transcription and pre-mRNA splicing (11–14). In several genes, TDP-43 has been shown to bind directly to pre-mRNAs and regulate their splicing (12,13,15–18). In fact, widespread dysregulation of pre-mRNA splicing has been demonstrated in TDP-43-depleted cultured cells, TDP-43-depleted mouse brain and affected tissues from ALS patients (12,13,17–20). These results suggest that dysregulation of pre-mRNA splicing is associated with ALS pathogenesis. However, this dysregulation is not fully explained by the fact that TDP-43 directly binds to and regulates pre-mRNA splicing.

*To whom correspondence should be addressed at: 1-757 Asahimachi-dori, Chuo-ku, Niigata-City, Niigata 951-8585, Japan. Tel: +81 252270684; Fax: +81 252270682; Email: onodera@bri.niigata-u.ac.jp
†These authors contributed equally to this work.

Pre-mRNA splicing is mainly regulated by the spliceosome, which is a complex of small nuclear ribonucleoproteins (snRNPs). Each snRNP contains one uridine-rich small nuclear RNA (U snRNA: U1, U2, U4, U5, U6, U11, U12, U4atac or U6atac) and associated proteins (21–23). Spliceosomes recognize the sequence for splicing junctions and branch sites (23,24). Based on the consensus sequence for the splicing junction, spliceosomes are classified into two classes: major spliceosomes (containing U1, U2, U4, U5 and U6) and minor spliceosomes (containing U11, U12, U5, U4atac and U6atac) (21,23). Most pre-mRNAs have introns that are spliced by the major spliceosome (U2-type intron), while a small number of pre-mRNAs have introns that are spliced by the minor spliceosome (U12-type intron) (21,23–25).

The biogenesis of spliceosomes is regulated in Gemini of coiled bodies (GEMs), which are molecularly defined by the presence of the survival of motor neuron (SMN) protein (26–28). TDP-43 associates with GEMs in cultured cells (4), suggesting that TDP-43 contributes to GEM formation or function. Indeed, in *TDP-43* transgenic or knockout mice, the number of GEMs has been positively correlated with the TDP-43 expression level (29). However, GEMs have not been fully evaluated in ALS spinal motor neurons. An association of GEMs and U snRNA with spinal motor neuron survival has been reported. Deletion of the *SMN* gene, the product of which is a major component of GEMs, causes spinal muscular atrophy (SMA) and decreases the number of GEMs in human tissues (30). In the *SMN* gene-deleted mouse, the number of GEMs and the levels of U snRNAs and U snRNA–protein complexes decrease (31–34). Here, we investigated the effect of TDP-43 depletion on the formation and function of GEMs in terms of U snRNA levels in cultured cells. We further investigated GEMs, U snRNA levels and pre-mRNA splicing in tissues affected by ALS to elucidate whether GEMs are associated with the molecular pathogenesis of ALS.

RESULTS

Decreased number of GEMs in TDP-43-depleted cultured cells

We investigated the intranuclear localization of TDP-43 foci in HeLa cells and observed that a subset of TDP-43 foci was located near GEMs, as reported by Wang *et al.* (Fig. 1A) (4). To investigate whether TDP-43 affects the formation of GEMs, we investigated the number of GEMs in cells treated with TDP-43 or control siRNA. In HeLa cells treated with TDP-43 siRNA, the level of TDP-43 expression was reduced to less than 10% of that in HeLa cells treated with control siRNA (Fig. 2A). The number of GEMs (mean $\pm$ SD) was significantly decreased in HeLa cells treated with TDP-43 siRNA (1.30 ± 1.33) compared with controls (2.64 ± 1.68; $P < 0.001$) (Fig. 1B and C). In addition, the size of GEMs was also significantly decreased in cells treated with TDP-43 siRNA (Fig. 1D). However, the effect of decreasing TDP-43 on the size of GEMs (decreased to 12% of the control) is relatively smaller than the effect on the number of GEMs (decreased to 59% of the control). To exclude the possibility that decreased cell viability results in a reduced number of GEMs, we investigated cell viability. However, we found that cell viability is not significantly reduced in cells treated with TDP-43 siRNA (Fig. 1E). We further evaluated the effects of TDP-43 on the number of GEMs in TDP-43 overexpressed cells. The number of GEMs (mean $\pm$ SD) was significantly decreased in HeLa cells transfected with TDP-43 cDNA (0.86 ± 0.10) compared with controls (1.59 ± 0.11; $P < 0.001$) (Supplementary Material, Fig. S1).

Decreased SMN complex proteins in TDP-43-depleted cultured cells

To investigate the mechanism that reduces the number of GEMs in TDP-43-depleted cells, we investigated the protein–protein interaction between TDP-43 and GEM component proteins. However, as previously reported, TDP-43 did not co-immunoprecipitate with GEM component proteins (Supplementary Material, Fig. S2) (14). Decreasing the quantity of component proteins of GEMs leads to a diminished number of GEMs (27,35). Therefore, we investigated the levels of component proteins of GEMs, including SMN and Gemin2, 3, 4, 6 and 8 in HeLa and SH-SY5Y cells treated with TDP-43 siRNA (Fig. 2A–C). We observed a severe reduction in SMN (decreased to 40.8% in HeLa and 41.0% in SH-SY5Y of control levels; $P < 0.005$), Gemin6 (decreased to 76% in HeLa and 64% in SH-SY5Y of control levels; $P < 0.05$) and Gemin8 (decreased to 45% in HeLa and 57% in SH-SY5Y of control levels; $P < 0.005$). In addition, Gemin3 (decreased to 74% of control levels in SH-SY5Y; $P < 0.05$) and Gemin4 (decreased to 89% of control levels in HeLa; $P < 0.05$) were also slightly decreased compared with control levels. To exclude the possibility that reduction in the amounts of these proteins resulted from off-target effects of the siRNA, we further performed the same experiment with four additional RNAi sequences targeted to the 3′ UTR of *TDP-43* mRNA (Fig. 2D). The amounts of SMN, Gemin3, Gemin6 and Gemin8 decreased proportionally to the amount of TDP-43 (Fig. 2D). A similar result was obtained in SH-SY5Y cells (Supplementary Material, Fig. S3).

To explore the mechanism by which depletion of TDP-43 reduces the SMN level, we used quantitative reverse transcription polymerase chain reaction (qRT-PCR) to investigate *SMN* mRNA levels. TDP-43 has been suggested to enhance inclusion of exon 7 in the *SMN2* gene (15), a second copy of the *SMN* gene. *SMN2* contains a single-nucleotide polymorphism in exon 7 that enhances exclusion of exon 7 and consequently produces unstable SMN protein (28). Therefore, we hypothesized that reduction in TDP-43 may enhance exclusion of exon 7 in the *SMN2* gene, leading to a decreased amount of SMN protein. However, we did not observe an increase in the exclusion of exon 7 in *SMN* mRNA (Fig. 2E and F). Moreover, we did not observe the additional aberrant alternative splicing variants in TDP-43-depleted cells (Supplementary Material, Fig. S4A and B). In contrast, we observed that all SMN splicing variants were decreased to half of the mRNA levels of control cells (Fig. 2F). The amounts of *Gemin2, 3* and *8* mRNA, which directly bind to SMN protein (36), were not altered in TDP-43-depleted cells (Supplementary Material, Fig. S4C). We further investigated whether the reduction in SMN expression was influenced by other proteins associated with splicing, including hnRNP A1, H1 and FUS. The expression levels of *SMN* mRNA were significantly decreased by FUS and hnRNP H1 siRNA, but not by hnRNP A1 siRNA. However, the effect

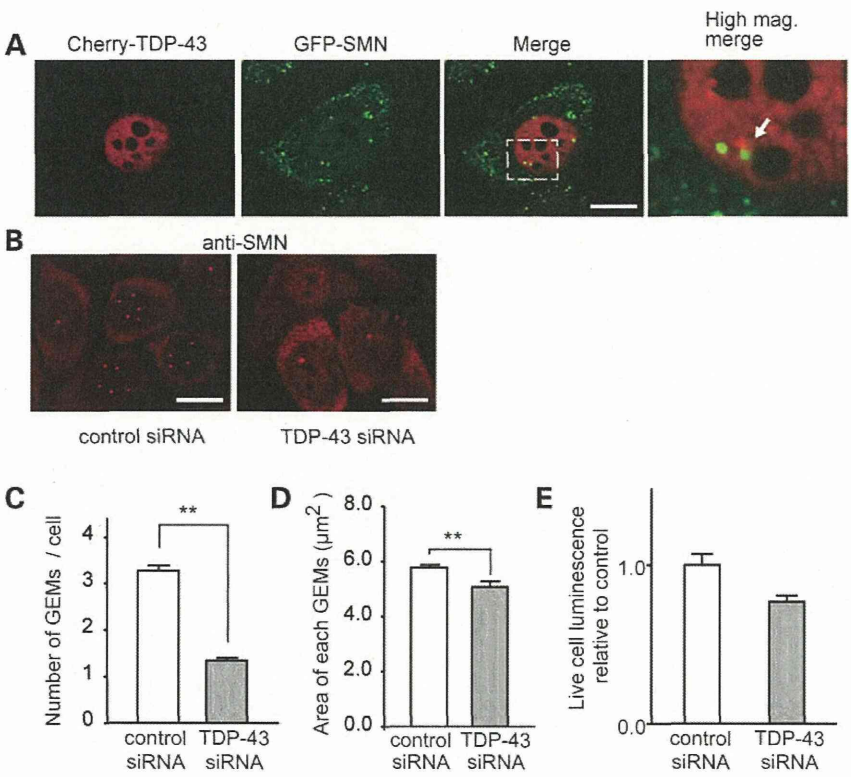

Figure 1. Decreased number of GEMs in TDP-43-depleted HeLa cells. (**A**) HeLa cells were transfected with both pmCherry-tagged TDP-43 and GFP-tagged SMN. The right image is a magnified image of the area indicated with dashed lines in the merged image. TDP-43 was localized near SMN in the nucleoplasm (arrow). (**B**) Immunocytochemistry analysis of GEMs in HeLa cells treated with non-targeting control or TDP-43 siRNA. These cells were immunostained with an antibody directed against SMN (red). GEMs were visualized as red granules in the nucleus. (**C**) Quantitative analysis of the number of GEMs (number of cells = control siRNA: 221, TDP-43 siRNA: 184). (**D**) The area of each GEM (number of counted GEMs = control: 709, TDP-43 siRNA: 221). (**E**) The cell viability of TDP-43 siRNA-treated HeLa cells using the CytoTox-Glo™ Cytotoxicity Assay. The data are presented as a ratio of the viability observed with control siRNA ($n = 4$). (D and E) In a bar graph, data represent the mean with standard error. The statistical comparisons were performed using the Mann–Whitney U test. $^{**}P < 0.001$; scale bars: 10 μm (A and B).

of TDP-43 siRNA was more severe compared with the other proteins (Supplementary Material, Fig. S5).

Decreased number of GEMs in spinal motor neurons from patients with ALS

Next, we investigated the number of GEMs in spinal motor neurons of ALS patients. We observed a subset of GEMs attached to TDP-43-immunopositive foci (Fig. 3A–H, Supplementary Material, Fig. S6A–D). We obtained three-dimensional reconstructed surface images of GEMs from Z-stacks of confocal images of spinal motor neuron nuclei (Fig. 4A) and compared the number of GEMs in ALS patients and controls (Fig. 4B). The number of GEMs per nucleus (mean ± SD) was significantly decreased in neurons from sporadic ALS patients compared with controls (3.25 ± 1.40 in ALS, 11.05 ± 2.14 in controls; $P < 0.05$) (Figs 3E–L and 4C, Supplementary Material, Fig. S6C–F and I–L).

We further investigated the number of GEMs in motor neurons from one familial ALS case carrying a p.Gln343Arg mutation in *TDP-43* (3) and one familial ALS case carrying a p.Asp101Tyr mutation in *SOD1* (37) (Fig. 3M–T). We found that the mean number of GEMs was also decreased (2.67 ± 0.50: mean ± SE) in the familial ALS case carrying a p.Gln343Arg mutation in *TDP-43* (3) but not in the familial ALS case carrying a p.Asp101Tyr mutation in *SOD1* (14.33 ± 1.90: mean ± SE) (Fig. 4B). We subsequently compared the number of GEMs with or without nuclear TDP-43. The number of GEMs (mean ± SD) was similar between motor neurons with or without nuclear TDP-43 (3.03 ± 1.40 in neurons with nuclear TDP-43, 3.02 ± 1.99 in neurons without nuclear TDP-43) (Figs 3E–L and 4D, Supplementary Material, Fig. S6C–F and I–L). The volume of GEMs (mean ± SD) did not differ significantly between the neurons from ALS patients and controls (0.60 ± 0.20 μm^3 in ALS, 0.67 ± 0.32 μm^3 in controls) (Fig. 4E).

We also used anti-coilin antibody to compare the number of Cajal bodies, which are associated with TDP-43 and GEMs, in spinal motor neurons of ALS patients and controls (4). The number of Cajal bodies per nucleus (mean ± SD) was significantly decreased in the neurons from sporadic ALS patients compared with controls (6.35 ± 1.69 in ALS, 15.33 ± 1.59 in controls; $P < 0.05$) (Fig. 4F and G).

Alteration of the U snRNA repertoire in TDP-43-depleted cells

GEM plays an important role in the biogenesis of U snRNA–protein complexes, a component of pre-mRNA splicing

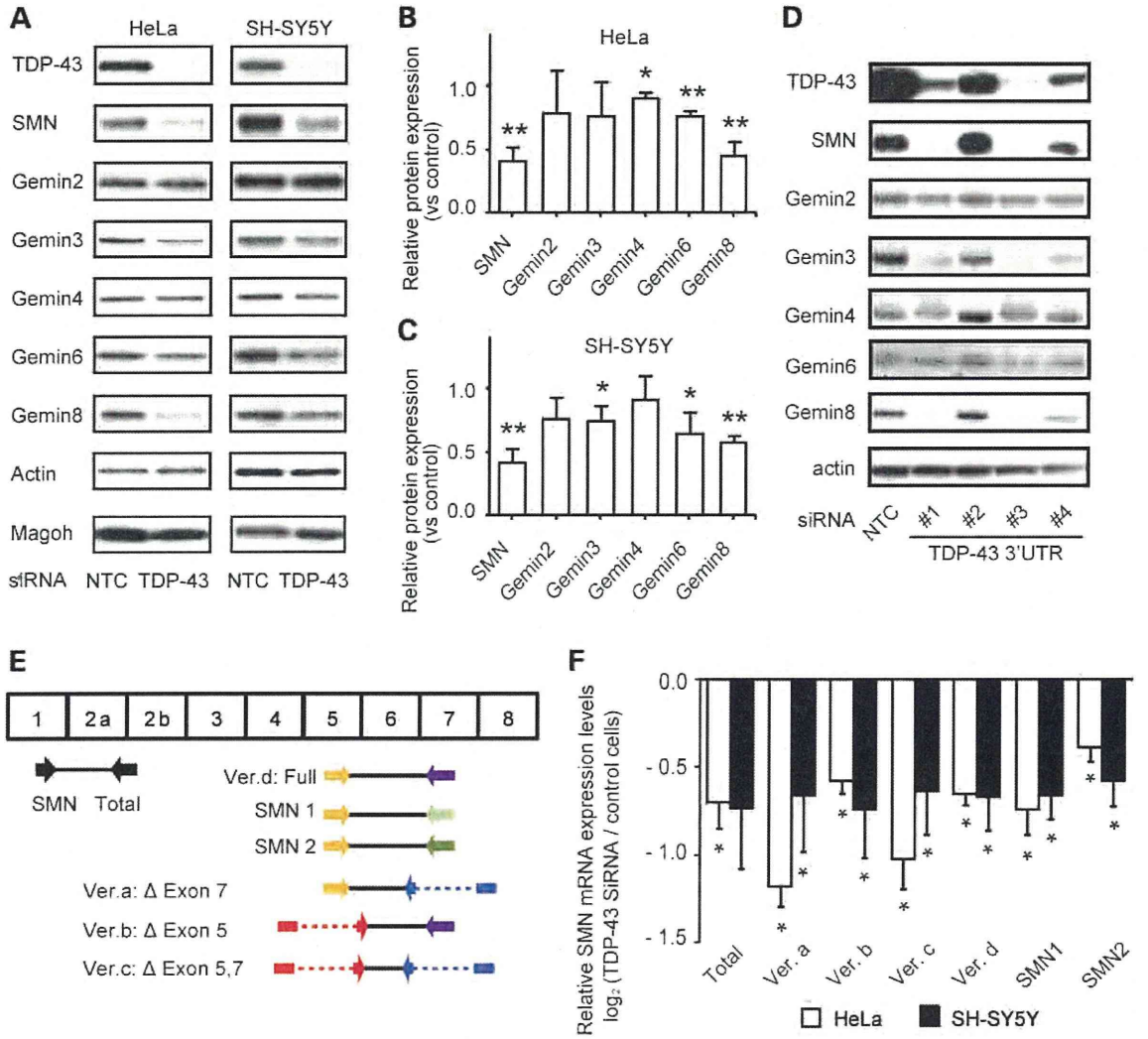

Figure 2. Decrease in SMN complex proteins in TDP-43-depleted HeLa and SH-SY5Y cells. (**A**) Total protein extracts were prepared from cells treated with control or TDP-43 siRNA. SMN and Gemin proteins were detected by quantitative immunoblot, using β-actin and Magoh as loading controls. (**B** and **C**) The relative amount of SMN and Gemin proteins in cells treated with TDP-43 siRNA. (B) HeLa; (C) SH-SH5Y cells. Data represent the mean with standard deviation from three independent experiments. Statistical comparisons were performed with Student's *t*-test. $^{*}P < 0.05$; $^{**}P < 0.005$. (**D**) Total protein extracts were prepared from HeLa cells treated with one of four different 3′ UTR TDP-43 siRNAs (#1–4). SMN and Gemin proteins were detected by quantitative immunoblot using β-actin as a loading control. (**E** and **F**) Quantification of *SMN* mRNA levels in TDP-43-depleted cultured cells. (E) A schematic indicating *SMN* mRNA and the positions of the primers that were used in real-time qRT-PCR assays. The exons are indicated by white boxes. The arrows and lines indicate the amplification primers and the amplified products for the *SMN* mRNA quantification assay. (F) Quantification of *SMN* mRNA in TDP-43-depleted cells (HeLa cells as white bars and SH-SY5Y cells as black bars). The normalization factor was calculated from the results of two endogenous controls, *PPIA* and *TBP* in HeLa cells, and *RPLP1* and *RPS18* in SH-SY5Y cells. These genes were selected as controls from among 16 housekeeping genes (Takara) using the geNorm program (http://medgen.ugent.be/~jvdesomp/genorm/). Data represent the $\log_2$ mean values of the transcript ratios. The error bars show the standard error from three independent experiments. The error bars were calculated using the following formula: $\sqrt{[SE(control)]^2 + [SE(TDP - 43\ siRNA)]^2}$. The statistical comparisons were determined using REST2009 (http://www.gene-quantification. de/rest-2009.html). $^{*}P < 0.05$.

machinery (26–28). Thus, we investigated whether depletion of TDP-43 results in the reduction in U snRNA levels. Treatment with TDP-43-targeted siRNA reduced *TDP-43* mRNA levels to 10% in HeLa cells, 55% in SH-SY5Y cells and 8% in U87-MG cells relative to the levels observed in control cells. In HeLa cells, U5 and U12 snRNA levels were decreased to 70% of control levels, but this difference was not significant (Fig. 5A). In SH-SY5Y cells, U4atac and U6atac snRNA levels were significantly decreased to 61 and 85% of the levels observed in controls, respectively ($P < 0.05$) (Fig. 5B). In U87-MG cells, the U12 snRNA level was significantly decreased to 55% of the control level ($P < 0.05$), whereas U2, U6 and U11 snRNA levels were significantly increased ($P < 0.05$) (Fig. 5C). Because we had demonstrated that SMN is decreased in TDP-43-depleted cells, we then compared the levels of U snRNAs in SMN-depleted cells to investigate the possibility that these alterations resulted from the depletion of SMN. We observed that the repertoire of U snRNA in SMN-depleted

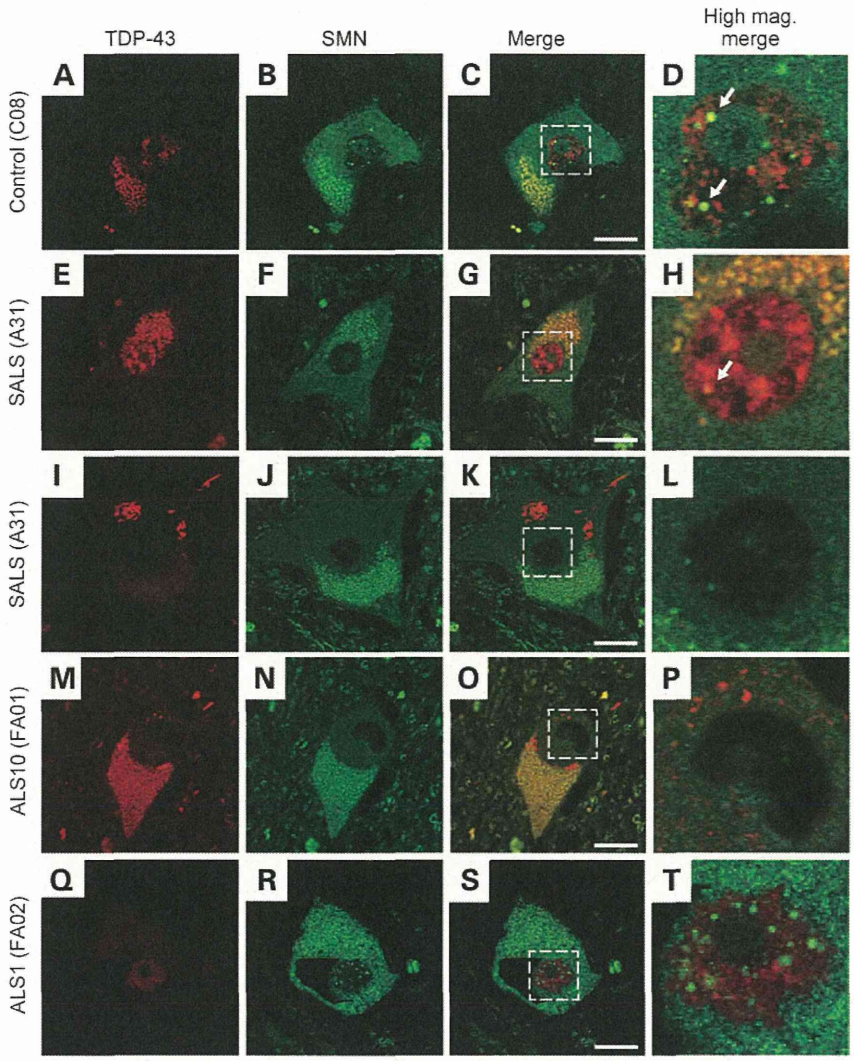

Figure 3. Decreased number of GEMs in spinal motor neurons of patients with ALS in two-dimensional images. Immunostaining of spinal motor neurons from control tissue (**A**–**D**), sporadic ALS cases (**E**–**L**), a familial ALS case carrying a p.Gln343Arg mutation in *TDP-43* (**M**–**P**) and a familial ALS case carrying a p.Asp101Tyr mutation in *SOD-1* (**Q**–**T**) was performed using anti-TDP-43 (red) and anti-SMN antibodies (green) and observed with confocal microscopy. Panels A–H and Q–T show normal nuclear TDP-43 staining, and panels I–P show TDP-43-positive skein-like inclusions in the cytoplasm. A subset of TDP-43 loci co-localized to GEMs (arrow). The images on the right (D, H, L, P and T) are magnified images of the area indicated with dashed lines in the merged images (C, G, K, O and S). The numbers correspond to the case number described in Supplementary Material, Tables S2 and S3. Scale bar: 20 μm.

HeLa cells differed from that in TDP-43-depleted HeLa cells (32,33). Moreover, the repertoire of U snRNA in SMN-depleted U87-MG cells was not similar to that observed in TDP-43-depleted U87-MG cells (Fig. 5C and D). These results indicate that the alteration of U snRNA in TDP-43-depleted cells does not simply result from the depletion of SMN.

U12 snRNA level was decreased in tissues from patients with ALS

We next investigated U snRNA levels in the spinal cord, motor cortex, thalamus, cerebellar hemisphere, kidney, skeletal muscle and liver tissues of patients with ALS and controls. The spinal cord and motor cortex were selected as regions with TDP-43 pathology, the thalamus was selected as a non-motor region with TDP-43 pathology and the cerebellar hemisphere was selected as a region in which TDP-43 pathology has never been observed (38). U12 snRNA was significantly decreased in the spinal cord (to 82%), motor cortex (to 82%) and thalamus (to 67%) of ALS patients compared with the corresponding control tissues ($P < 0.05$) (Figs 6A–C). Additionally, in the spinal cord of patients with ALS, both U6 and U11 snRNA levels were significantly decreased to 74 and 75% of the levels that were detected in control tissue, respectively ($P < 0.05$) (Fig. 6A). The U6atac level was significantly decreased ($P < 0.05$) in the motor cortex (to 78% of control levels) and the thalamus (to 70% of control levels) (Fig. 6B and C). In contrast, no significant difference in U snRNA was demonstrated in the cerebellum, skeletal muscle or kidneys (Figs 6D–F). In the liver of ALS patients, U11 and U6atac

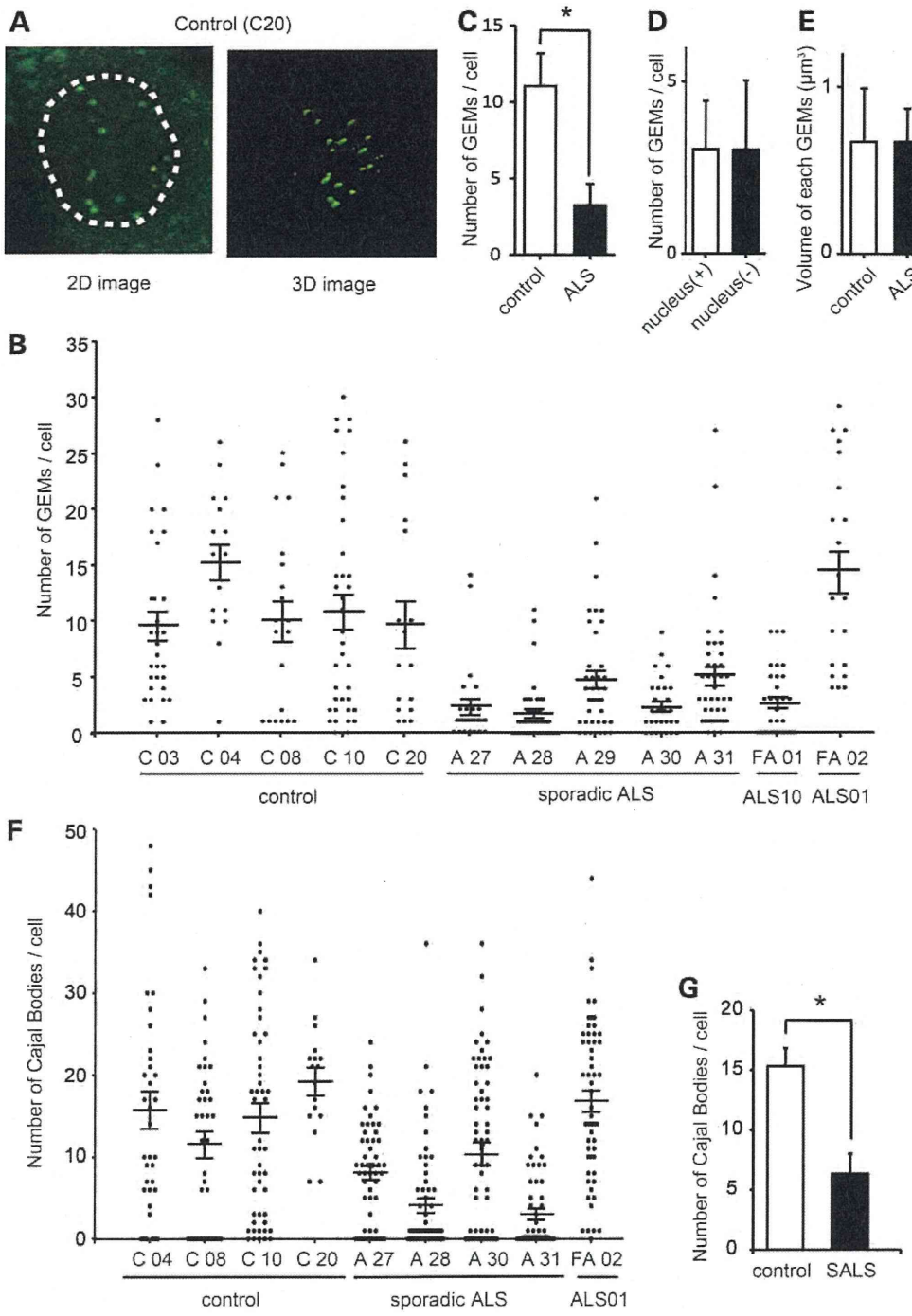

Figure 4. Decreased number of GEMs in spinal motor neurons of ALS patients in three-dimensional surface images. (**A**) The two-dimensional (left) and three-dimensional surface (right) images of GEMs in spinal motor neurons. The dashed line indicates the area of the nucleus. Serial z-section images were acquired with a confocal laser-scanning microscope using anti-SMN antibodies (green), and three-dimensional surface modules were constructed using Imaris software. (**B**) Scattergram of the total number of GEMs in the examined spinal motor neurons. The total number of GEMs per spinal motor neuron from each individual was plotted ($n = 16–42$). The numbers labeled in the x-axis correspond to the case numbers (described in Supplementary Material, Tables S2, S3). The lines and error bars represent the mean ± SEM. (**C**) The number of GEMs in each spinal motor neuron from controls ($n = 5$) and ALS patients ($n = 5$). (**D**) The number of GEMs in each spinal motor neuron with or without nuclear TDP-43 from ALS patients ($n = 5$). (**E**) The volume of each GEM in spinal motor neurons from controls ($n = 5$) and ALS patients ($n = 5$). (C–E) Data represent the mean with standard deviation. The statistical comparisons were performed using the Mann–Whitney U test. $^*P < 0.05$.

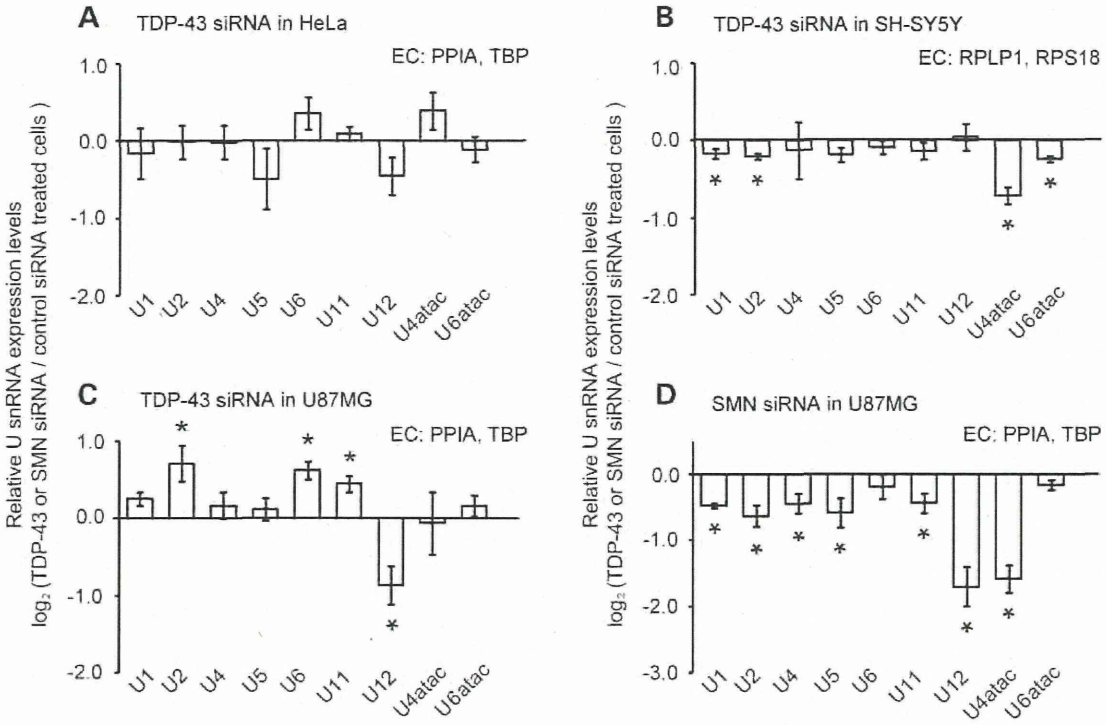

Figure 5. Decreased U snRNA levels in TDP-43-depleted cells. Quantitative RT-PCR was used to assay the U snRNA levels in cells treated with control, TDP-43 or SMN siRNAs. The ratios of the snRNA levels that were detected in TDP-43- or SMN-depleted cells compared with those observed in control cells were measured. TDP-43 siRNA-treated (**A**) HeLa, (**B**) SH-SH5Y and (**C**) U87-MG cells. (**D**) U87-MG cells transfected with SMN siRNA. The error bars were calculated as in Figure 2F. The normalization factor was calculated from the results of two endogenous controls, *PPIA* and *TBP* in HeLa and U87-MG cells, and *RPLP1* and *RPS18* in SH-SY5Y cells. Data represent the $\log_2$ mean values of the transcript ratios. The error bars show the standard error from three independent experiments. The statistical comparisons were determined using REST2009 (http://www.gene-quantification.de/ rest-2009.html) $^*P < 0.05$.

levels were significantly decreased to 54 and 28% of the levels observed in controls, respectively ($P < 0.05$) (Supplementary Material, Fig. S7). *SMN* mRNA levels were not decreased in the tissues of ALS patients (Supplementary Material, Fig. S8).

Decreased U12-type snRNPs in ALS spinal motor neuron

To show the reduction in U12 snRNA and a minor spliceosome in spinal motor neurons, we next investigated the amounts of U11/12-type spliceosome in spinal motor neurons of ALS patients using immunofluorescent staining with anti-small nuclear ribonucleotide protein 59 kDa (snRNP 59 K) antibody. snRNP 59 K is a component of the U11/U12-type spliceosome (39). Although the normal spinal motor neuron is well stained with the antibody (Fig. 7A–C), the nucleus of neurons from ALS patients does not stain well with the antibody (Fig. 7D–F). The fluorescence intensity of snRNP 59 K in the nucleus of each motor neuron in which TDP-43 still remained was significantly decreased in ALS patients compared with controls (Fig. 7G, Supplementary Material, Fig. S9).

Finally, we investigated splicing efficiencies of the U2- and U12-type intron in *Ipo4*, *IFT80* and *GARS* genes by qRT-PCR analysis using RNA samples isolated from TDP-43-depleted cells or tissues affected by ALS (Supplementary Material, Fig. S10) (40,41). TDP-43-depleted U87-MG and SHSY-5Y cells showed a decrease in the mRNA of *Ipo40* and *GARS* with a spliced U12-type intron. TDP-43-depleted U87-MG cells showed an increase in the mRNA of *Ipo4* and *IFT80* with a retained U12-type intron. Furthermore, in ALS motor cortex, the mRNA of *Ipo4* with a spliced U12-type intron significantly decreased, whereas the mRNA of *Ipo4* with a retained U12-type intron tended to increase compared with controls. In contrast, in tissues with SOD1 mutations, mRNA of *Ipo4* and *GARS* with retained introns tended to decrease (Supplementary Material, Fig. S11). However, TDP-43-depleted U87-MG cells also showed an increase in mRNA of *Ipo4*, *IFT80* and *GARS* genes with a retained U2-type intron.

DISCUSSION

Here, we have shown a decrease in the number of GEMs in TDP-43-depleted cultured cells and spinal motor neurons of patients with ALS. These findings are consistent with the results obtained from gene-modified mice: the number of GEMs increased in the TDP-43 transgenic mouse, and no GEMs were observed in the TDP-43 knockout mouse (29). In addition, we observed a decrease in the levels of U12 snRNA in tissues from ALS patients with TDP-43 pathology but not in tissues without TDP-43 pathology. Finally, we found a decrease in U11/U12-type snRNPs in spinal motor neurons from patients with ALS. GEMs participate in U snRNA assembly, maturation, expression and recycling of a fraction of U snRNPs (27,28,42). Indeed, in SMA model mice, depletion of SMN, which is a

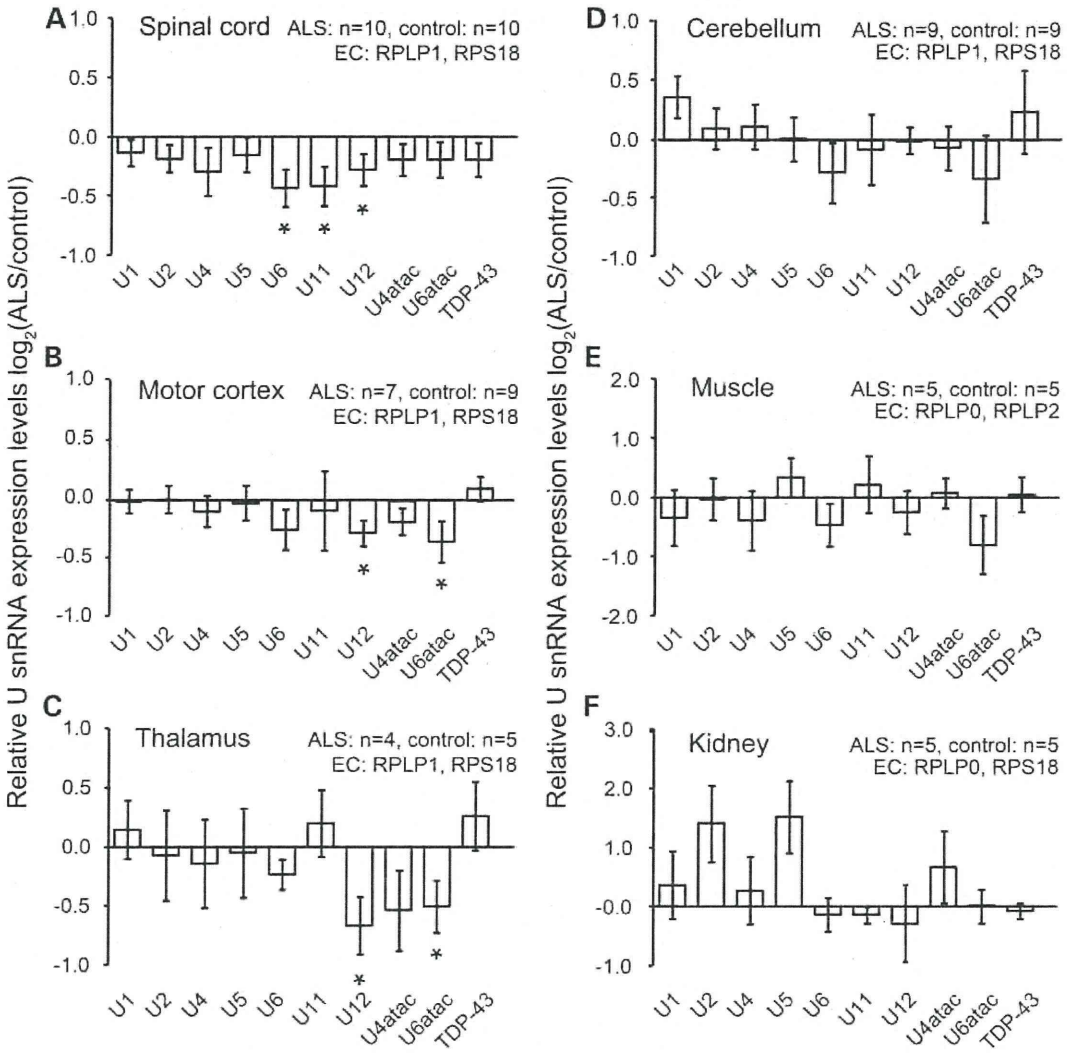

Figure 6. Decreased U snRNA levels in the affected tissues of ALS patients. Total RNA was purified from (**A**) spinal cord, (**B**) motor cortex, (**C**) thalamus, (**D**) cerebellum, (**E**) muscle and (**F**) kidney samples from patients with ALS ($n = 4–10$) and controls ($n = 5–10$). Real-time qRT-PCR analyses were performed to determine the relative levels of 9 U snRNAs and *TDP-43* mRNA in each tissue. The normalization factor was calculated from the mRNA levels of two endogenous controls (EC), *RPLP1* and *RPS18* in (A–D), *RPLP0* and *RPLP2* in (E) and *RPLP0* and *RPS18* in (F). These genes were selected as endogenous control genes as described in Figure 2F. Data represent the $\log_2$ mean values of the transcript ratios. The error bars show the standard error from at least four independent experiments. The error bars were calculated as described in Figure 2F. The statistical analyses were performed using the REST2009 program (http://www.gene-quantification.de/rest-2009.html) $^*P < 0.05$.

major component of GEMs, decreased the levels of U11 and U12 snRNAs (32,33). Thus, we can speculate that the decreased number of GEM results in a reduction in U12 snRNA and U11/U12-type spliceosome. Taken together, these findings raise the possibility that disturbance of pre-mRNA metabolism regulated by the U11/U12-type spliceosome may underlie the pathogenesis of ALS. Although these results are not convincing, the decreased expression of mRNA with a spliced U12-type intron in TDP-43-depleted U87-MG cells and ALS motor cortex supports this hypothesis.

Based on the consensus sequence for the splicing junction, U snRNAs are divided into two classes: major spliceosomes (U1, U2, U4, U5 and U6) and minor spliceosomes (U11, U12, U5, U4atac and U6atac) (21,23). Although GEMs associate with all types of U snRNAs, U12 snRNA was preferentially decreased in tissues with TDP-43 pathology. Similarly, in the global SMN-deficient mouse, U11 and U12 snRNA preferentially decreased in the affected tissues (32,33). Both U11 and U12 snRNA belong to the minor spliceosome class. The preferential decrease in minor spliceosome U snRNA, compared with major spliceosome U snRNA, is partially explained by the difference in the number of genes for each U snRNA. Multiple genes encode U1 and U2 snRNA, whereas a single gene encodes U11 and U12 snRNA (43). Therefore, decreasing the number of GEMs associated with U snRNA transcription may have a greater influence on single-gene than multiple-gene U snRNAs (43).

Both U11 snRNA and U12 snRNA participate in generation of the pre-mRNA lariat structure to select the donor and acceptor